Proceedings of the 21st ICSMGE, Vienna, Austria, 14 – 19 June 2026. Pistrol, Adam & Schweiger (eds.)
Published by: ÖGG, Austrian Society for Geomechanics, Salzburg, Austria, ISBN 978-3-9503898-4-5
https://doi.org/10.53243/ICSMGE2026-1520

Behavior of geotextile-encased columns under reloading: insights from centrifuge testing

Viktor Poberezhnyi, Oliver Detert
Engineering Department, HUESKER Synthetic GmbH, Gescher, Germany, poberezhnyi@huesker.de

Suzanne J.M. van Eekelen, Cihan Cengiz, Remco van den Berg
Geo-engineering, Deltares, Delft, The Netherlands

Steffen Taetz
Geotechnical Department, Ed. Züblin AG, Hamburg, Germany

Diethard König
Department of Civil and Environmental Engineering, Ruhr University Bochum, Bochum, Germany

ABSTRACT: This study examines the behavior of Geotextile Encased Columns (GECs) in soil foundation systems under reloading conditions. It focuses on the response of soft soil improved with GECs during loading, unloading, and reloading cycles, assessing possible changes in stiffness behavior. Building on di Prisco et al. (2006), who observed increased column stiffness during reloading in small-scale 1g tests, this research investigates the evolution of the GEC-to-soil stiffness ratio during unloading and reloading using centrifuge testing. During the tests, foil sensors registered the evolution of load distribution and a liquid levelling system monitored the settlement of the columns and the surrounding soil. Additionally, pore water pressure within the clay model was measured, capturing its response to loading cycles and the associated consolidation processes. Unlike previous studies on Ordinary Stone Columns (OSCs) and GECs, which focused on high-frequency cyclic loads like traffic or seismic events, this research examines single loading, unloading, and reloading cycles, simulating staged construction processes such as preloading, excavation and final construction. The findings provide valuable insights into GEC performance under variable loading, supporting the design of resilient geotechnical foundations.

KEYWORDS: Geotextile Encased Columns, Geosynthetics, Soil Improvement, Physical Modelling, Geotechnical Centrifuge.

1 INTRODUCTION

Geotextile-encased columns (GECs) have become an established solution for improving the load-bearing performance of soft soils, offering enhanced confinement, reduced settlements, and accelerated consolidation. Earlier, several researchers primarily focused on GECs subjected to monotonic or high-frequency cyclic loading, typical of traffic or seismic activity (Ardakani et al. 2018; Cengiz and Guler, 2018, 2020). Still, their behavior under staged loading and reloading cycles remains less understood, despite its practical relevance for construction processes involving preloading, partial removal, and final loading.

Earlier foundational studies, such as those by Raithel (1999), provided analytical and numerical models for GEC design, highlighting the significance of radial support and hoop tension forces. di Prisco et al. (2006) demonstrated in 1g model tests that partial unloading can increase system stiffness during reloading due to such effects as accumulation of plastic strains.

Building upon these concepts, the ELURPGEC project (Effect of Loading, Unloading and reloading on Geosynthetic Encased Columns; GEOLAB initiative) initiated centrifuge tests to investigate the evolution of GEC-to-soil stiffness ratios under staged loading conditions. Poberezhnyi et al. (2024) primarily focused on experimental methodology and scaling laws. The current article presents selected results and establishes a framework for interpreting the response of GEC systems under realistic loading scenarios.

This paper provides new insights into stress distribution and an approach for evaluating stiffness evolution in GEC foundations during loading, unloading, and reloading. By focusing on reloading after primary consolidation, distinct from high-frequency cyclic contexts, it contributes to the development of more resilient and adaptive GEC systems.

2 EXPERIMENTAL SETUP

2.1 *Geotechnical centrifuge*

In this research, experimental work was carried out in 2024 using the Deltares Actidyn C72-3 beam centrifuge located in Delft, Netherlands. Featuring a radius of 5 m and capable of supporting up to 260 t at 100g, it can simulate gravitational fields up to 150g (Zwaan et al., 2020).

2.2 *Model geometry*

Test setups (Figure 1 and Figure 2) were built in cylindrical steel containers (590 mm inner diameter) comprising, from bottom to top: a 90 mm base sand layer; a 250 mm foundation zone with GECs and clay; a leveling sand layer with basal reinforcement; a 90 mm top sand layer; and a water-pressurized cushion load actuator. The container was then closed with a top plate.

The GECs, measuring 40 mm in diameter, were fully embedded within the clay layer (240 mm). They were installed using the replacement installation method, filled with sand, and extended 10 mm into the top and 20 mm into the base sand layer, resulting in a total initial length of 270 mm. Two triangular GEC arrangements were tested: one with a 10% area ratio with 19 columns (Setup 1 shown in Figure 1 and applied in Test 3) and one with a 20% ratio with 37 columns (Setup 2 shown in Figure 2 and applied in Tests 1 and 2). Basal reinforcement was positioned on top of the foundation zone extending across the full surface area of the model. The basal reinforcement was fixed to a thermoplastic ring with high radial and low vertical bending stiffness. The loading system consisted of an actuator, employing a water-pressurized cushion to uniformly exert vertical surcharge.

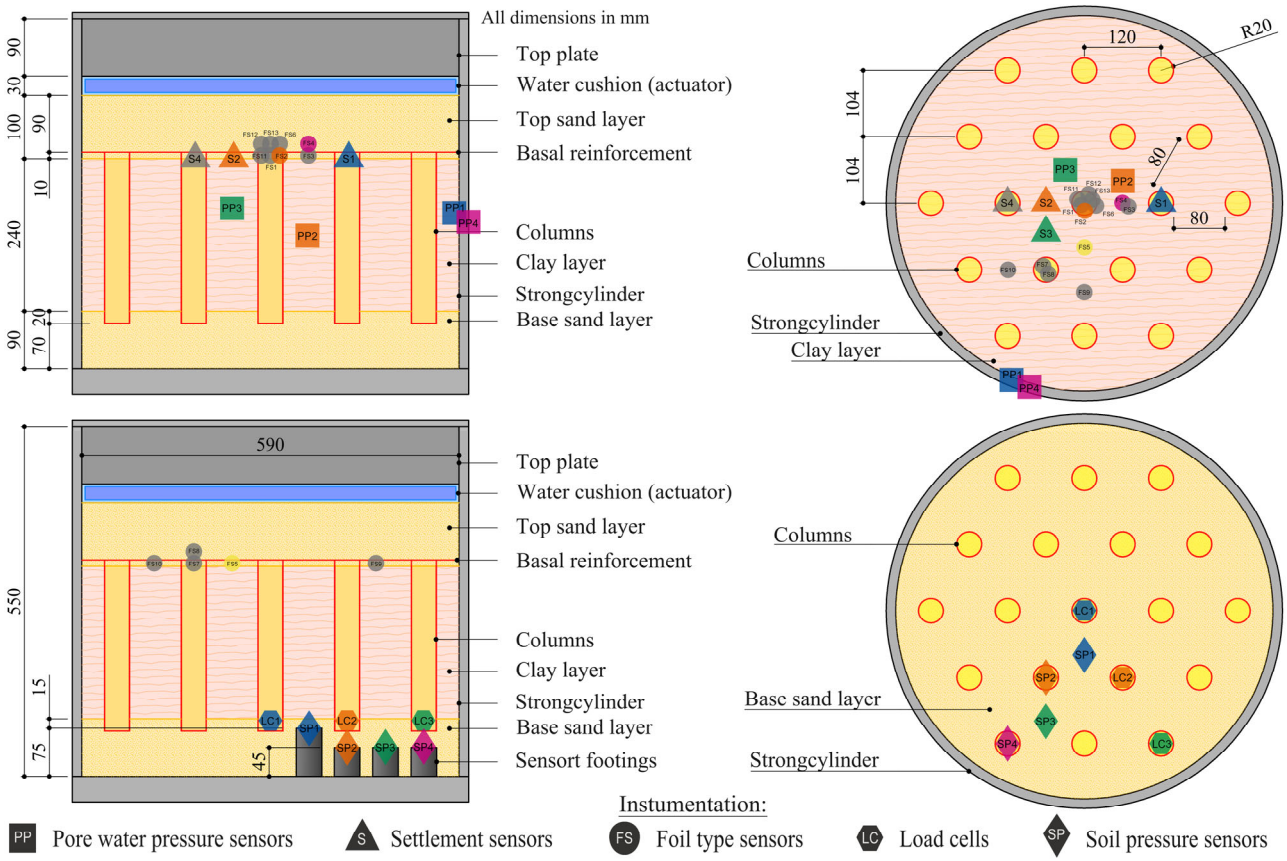

Figure 1. Setup 1 (Test 3; 10% area ratio, i.e., 19 GECs).

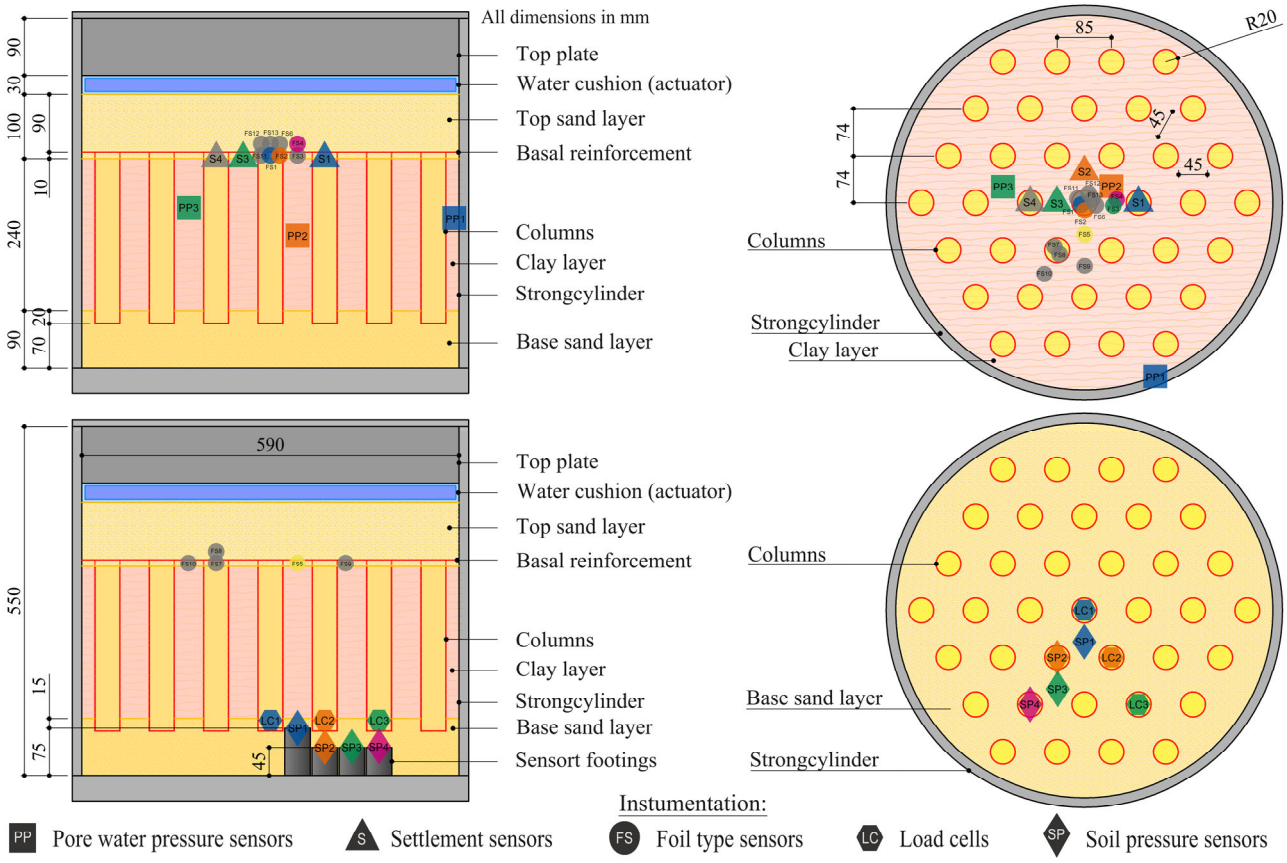

Figure 2. Setup 2 (Tests 1 and 2; 20% area ratio, i.e., 37 GECs).

2.3 *Scaling considerations*

The key scale factors for centrifuge modelling of GEC foundation systems derived from Viswanadham and König (2004), Caicedo et al. (2015), Reshma et al. (2019), and Dipankana and Viswanadham (2019), are listed in Table 1. The experiments were performed at a gravitational acceleration of 20 g (N=20), imposed at the surface of the clay layer.

Table 1. Key scale factors in centrifuge modelling

Parameter	Unit	Ng (model/prototype)
Classical dimensions		
Length	m	1/N
Load	kN	$1/N^2$
Stress	kPa	1
Mass	kg	$1/N^3$
Time (consolidation)	s	$1/N^2$
Strain	%	1
Density	kg/m³	1
Geosynthetic parameters		
Tensile load	kN/m	1/N
Secant stiffness modulus	kN/m	1/N
Tensile strength	kN/m	1/N
Strain	%	1

2.4 *Materials*

2.4.1 *Soil materials*

The clay layer consisted of Kaolin clay (KD 2000), commonly used in geotechnical modelling studies (Al-Tabbaa and Wood 1987; Sharma and Bolton 2020). Prior to the GEC installation, the clay layer underwent consolidation at 1g by applying a vertical stress of 40 kPa until reaching the targeted consolidation state. Following consolidation, it exhibited a liquid limit of 66% and plastic limit of 28%, an initial void ratio of 1.37, a saturated unit weight of 16.6 kN/m³, compression index of 0.276 and swelling index of 0.048.

The same type of uniformly graded fine silica sand (GEBA) with median grain size of 0.137 mm, uniformity and curvature coefficients of 1.35 and 1.12, respectively, was used for all sand layers and GEC fill.

2.4.2 *Textile materials*

The basal reinforcement consisted of a biaxial PP geotextile, attached at its edges to thermoplastic rings ensuring stability against pull-out. The column encasements were seamless sleeves, replicating those used in real projects. All geotextiles adhered to the scaling criteria (Poberezhnyi et al., 2024).

3 TEST PROGRAM

3.1 *Loading sequence*

The loading sequence consisted of distinct phases applied during testing. Initially, the model was accelerated to the target gravity level (20g) without additional loading, allowing initial consolidation under increased self-weight. Subsequently, a vertical surcharge load of approximately 100 kPa was applied, followed by a consolidation period. The next phase involved either complete unloading (to nearly 0% of the maximum load) or partial unloading (to 50% of the maximum load), with subsequent consolidation. Finally, the model underwent reloading to the full surcharge of approximately 100 kPa, again followed by consolidation. Figure 3shows the pressure applied to the top sand layer through the actuator over time in different tests.

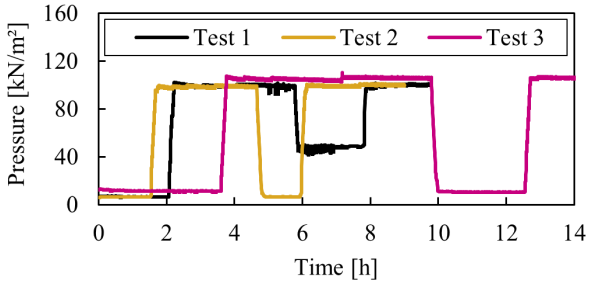

Figure 3. Pressure applied to the top sand layer through the actuator.

3.2 *Pre- and post-test 3D scanning*

High-resolution 3D laser scans captured precise surface coordinates before and after testing. Initially, scans were taken after the installation of columns and instrumentation, capturing the pre-test geometry. After testing, another 3D scanning recorded the post-test geometry. Comparing pre- and post-test scans enabled the precise evaluation of surface deformation. Although these scans were conducted at 1g rather than at the elevated g-level, they still provide valuable insights into the behaviour of the model and can be used to support the evaluation of deformation development of the GEC system.

Figure 4 illustrates the surface elevation changes at the top of the foundation zone by comparing two 3D scans, pre- and post-test (differences in mm). The color scale indicates the magnitude of surface elevation changes.

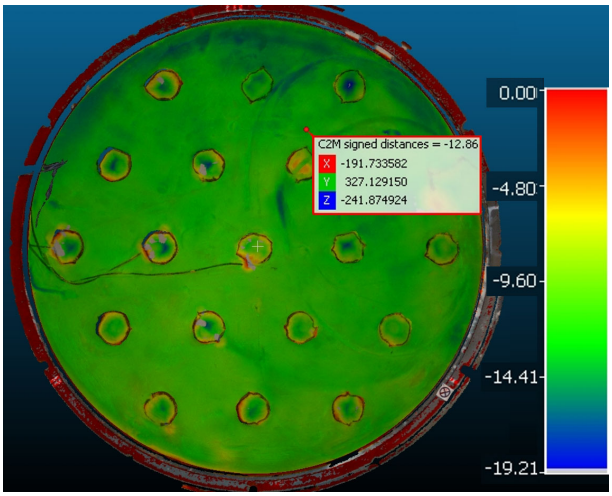

Figure 4. Difference between pre- and post-test surface elevation.

4 MEASUREMENT RESULTS

Due to space constraints, only selected test results are presented here. Note that some sensors (shown gray in Figure 1 and Figure 2) malfunctioned and yielded no usable data.

4.1 *Pore water pressure response*

Pore water pressures were measured using sensors installed in the clay between two or three central columns at depths of 80 mm (upper third of the clay layer) and 120 mm (mid-depth of the clay) from the clay surface. Additional sensors were mounted on the inner wall of the steel cylinder at a depth of 90 mm. Figure 5 shows the measured pore water pressures development over time for Test 3.

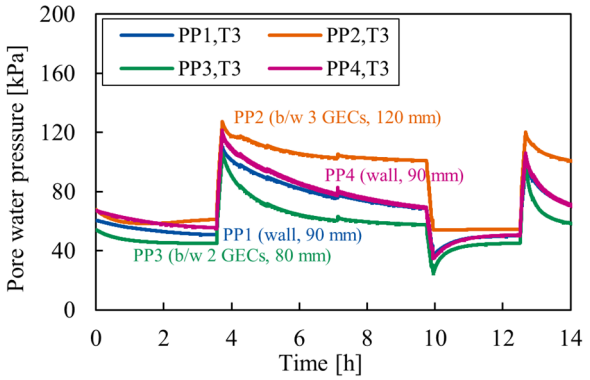

Figure 5. Pore water pressure development over time (Test 3).

4.2 *Vertical displacement measurements*

Settlements were measured both on the clay surface (between two or three central columns) and at the tops of the GECs. Shortly after reaching the target spin rate, the measured settlement on the GEC-head were zeroed to remove the initial column settlements induced by spin-up. Figure 6 shows the settlement development over time for Test 2.

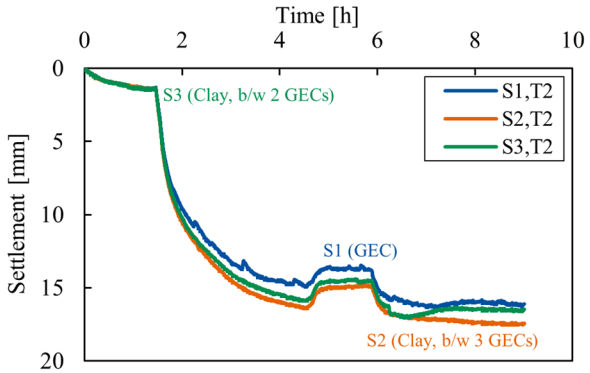

Figure 6. Settlement of GECs and clay surface (Test 2).

4.3 *Vertical stress measurements*

4.3.1 *At the foundation level*

Vertical stresses at the top of the foundation system were recorded by foil-type sensors installed both on the column heads and on the clay surface, placed above and below basal reinforcement (BR). The results shown in Figure 7 are from Test 1.

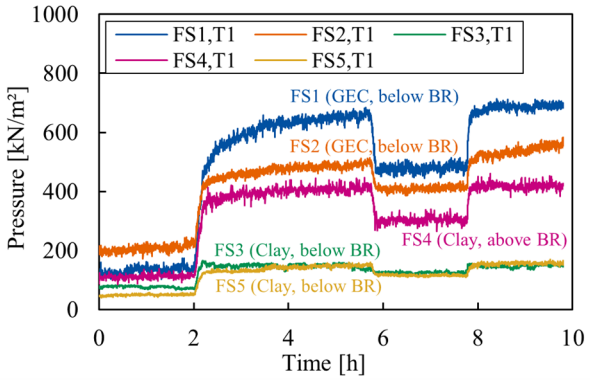

Figure 7. Vertical stresses over GECs and clay surface (Test 1).

4.3.2 *Within the base sand layer*

To capture vertical stresses below the GEC system, soil pressure sensors were installed in the base sand layer under GECs and at various depths under the clay. Figure 8 presents the results from Test 3. The higher load beneath the GECs compared to the clay results from load concentration on the GECs.

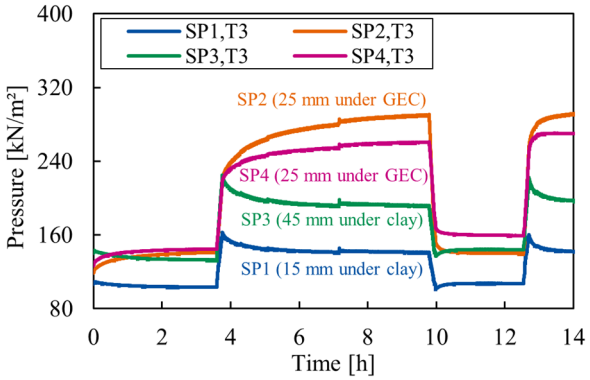

Figure 8. Vertical stress beneath GECs and clay (Test 3).

4.3.3 *At the GEC base*

Stresses were recorded by load cells installed at the base of the GECs. Figure 9 shows how the column position affects the vertical stresses at the column bases for Test 3. The graph differentiates between the central GEC (LC1), the mid-row 1 GECs (LC2), and the outer row 2 GECs (LC3), located closest to the strong cylinder walls. The results indicate that the central GEC carried the highest load, while those adjacent to the box wall carried the least. This pattern is likely influenced by interaction between the clay and the strong cylinder walls, which affects the second row of GECs most significantly.

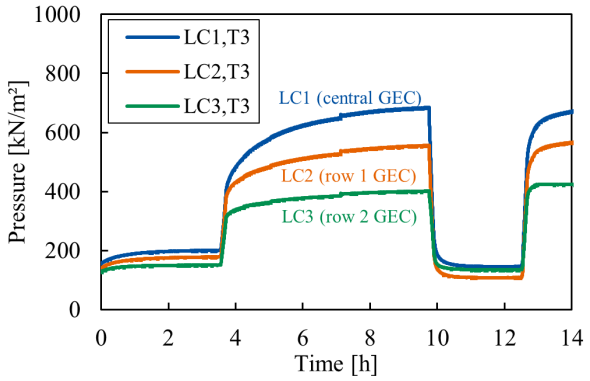

Figure 9. Vertical stresses at column bases (Test 3).

5 ESTIMATION OF RELOADING EFFECT

To quantify the influence of reloading on the response of GEC systems, we adopt an analytical approach that compares the vertical stress–settlement behavior during initial loading and subsequent reloading (after primary consolidation). The analytical procedure is detailed in the sub-sections below.

5.1 *Interpretation of vertical stress measurements*

Vertical stresses measured by foil type sensors at the top of the foundation system will be refined through a multi-stage conditioning process to minimize systematic and spatial biases.

The sensors provide readings at discrete sensor locations, which are inherently spatially heterogeneous. Values are typically higher at column centers than at their edges, and higher at the mid-span of three adjoining columns compared to the mid-span between two.

Therefore, accurate analysis requires position-dependent correction factors to reconcile these localized peaks with the true, area-averaged stress field. Such factors can only be quantified through a dedicated numerical calibration, for

example a three-dimensional finite-element back-analysis that models the sensor geometry, the stiffness contrast between column and clay, and the membrane action of the basal reinforcement.

In the absence of this calibration, the present analysis applies an interim procedure. Sensor signals are first split into above- and below- basal reinforcement datasets to account for basal reinforcement effects (see Section 6). Weighted spatial averaging is then applied only to measurements obtained beneath the basal reinforcement for each system component (GECs and clay). This yields a provisional but consistent estimate of the vertical stresses that truly act on the GECs and the clay.

5.2 *Estimation of vertical stress distribution and settlements*

Vertical stresses acting on the system components beneath the basal reinforcement, along with the corresponding settlements, are estimated for both loading and reloading stages. Only values recorded after primary consolidation are considered, ensuring that transient effects are excluded.

5.3 *Calculation of apparent vertical stiffness*

For each component and each loading cycle, the apparent stiffness $K_{i,j}$ (kN/m^3) is defined as the ratio of vertical stress to the corresponding settlement, as generally expressed in Equation (1).

$$K_{i\in\{GEC,clay\},j\in\{loading,reloading\}} = \frac{\sigma_{v,i,j}}{s_{i,j}} \quad (1)$$

5.4 *Derivation of stiffness ratios*

To evaluate the relative mechanical response of GECs and the clay, stiffness ratios RK_j are introduced. These ratios allow for a direct comparison of the deformation behavior of system components under loading and reloading conditions.

The apparent stiffness values are computed separately for the initial loading phase and for the reloading phase. Based on these values, the stiffness ratio RK_j is defined as the ratio of the apparent vertical stiffness of GECs to that of clay for different stages of loading, as expressed in Equations (2) and (3).

$$RK_{loading} = \frac{K_{GEC,loading}}{K_{clay,loading}} \quad (2)$$

$$RK_{reloading} = \frac{K_{GEC,reloading}}{K_{clay,reloading}} \quad (3)$$

5.5 *Assessment of reloading effects*

By comparing $RK_{loading}$ and $RK_{reloading}$, it is possible to assess the effect of reloading on the performance of the GEC system. An increase in this ratio from loading to reloading suggests that GECs exhibit a greater relative stiffness upon reloading, potentially due to accumulated plastic strains, enhanced confinement effects, or other effects.

5.6 *Design implications for GEC systems*

There are two common approaches to design basal reinforcement in GEC foundation systems. The first method, widely used for geotextile-encased column (GEC) systems, is based on global stability analyses such as Bishop's slip-circle method. This approach assumes that the stiffness of the supporting elements (e.g., GECs) and the surrounding soft soil is relatively uniform.

This occurs when there is a significant stiffness difference between the support elements (e.g., piles or columns) and the adjacent soil, causing downward vertical deflection of the basal reinforcement in the mid-span and resulting in tensile forces within it.

Although current design codes (e.g. EBGEO 2011) offer stiffness-ratio thresholds as a guideline for applying the membrane design method, multiple additional factors such as the area replacement ratio and stiffness of the soft subsoil can significantly influence basal reinforcement behaviour.

For example, while a global stability analysis may be suitable for stiffer soils, a membrane design approach might become relevant for softer soils, even if the column layout is the same.

Therefore, further research is essential to clarify under what specific conditions the global stability approach or the membrane design more accurately reflects the forces developing within basal reinforcement. Additionally, investigations should address how potential changes in stiffness ratios due to reloading effects, such as those from staged construction processes, impact the selection of an appropriate design approach.

6 EFFECT OF BASAL REINFORCEMENT ON STRESS DISTRIBUTION

Basal reinforcement (BR) placed above the foundation level plays a key role in redistributing vertical stresses in GEC systems. It redirects load from the soil to the columns, thereby reducing stress on the clay and increasing it on the columns.

Due to this effect, vertical stresses on the clay beneath the basal reinforcement are typically lower than those above, while the opposite is true for columns. This behavior indicates that basal reinforcement effectively captures and transfers loads to the columns, improving the efficiency of the foundation system.

Figure 10 and Figure 11 present the development of vertical stresses over time, based on measurements from sensors placed on clay below and above basal reinforcement across multiple tests. The data consistently show lower stresses in the clay beneath the reinforcement compared to those above, highlighting the role of basal reinforcement in efficient load transfer.

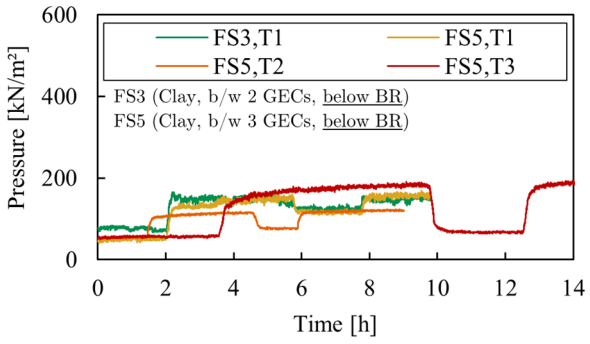

Figure 10. Vertical stresses on clay below basal reinforcement.

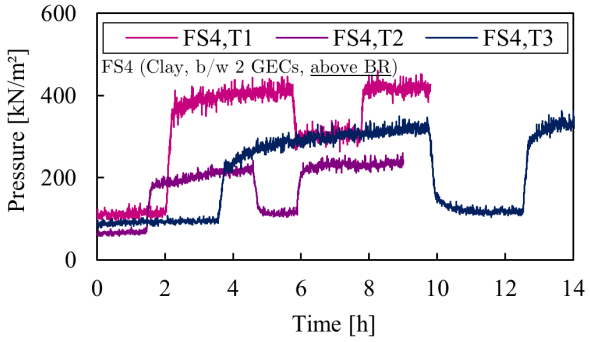

Figure 11. Vertical stresses on clay above basal reinforcement.

7 CONCLUSIONS

This study presents centrifuge model experiments investigating the response of geotextile-encased column (GEC) systems subjected to staged loading, including unloading and reloading phases. The tests were designed to simulate realistic construction scenarios such as preloading, partial removal, and final conditions not typically addressed in studies focused on high-frequency cyclic or monotonic loading.

The results provide a comprehensive dataset on load redistribution, settlements, and pore pressure behavior in GEC-improved soft soils under vertical reloading after primary consolidation. Emphasis was placed on characterizing the stress transfer mechanisms within the system, particularly in relation to the role of the basal reinforcement and the interaction between columns and surrounding soil.

An interpretative framework for the experimental results is proposed, supported by selected findings from instrumentation and observations. The analysis includes a focus on how the basal reinforcement affects the stress distribution within the foundation system.

Ongoing and future work will aim to expand upon these observations and contribute to a broader understanding of GEC behavior under variable loading conditions. The experimental results serve as a basis for further interpretation, numerical modeling, and discussion.

8 ACKNOWLEDGEMENTS

The authors gratefully acknowledge the financial support provided by the European Union's Horizon 2020 research and innovation program under Grant Agreement No. 101006512 for the transnational GEOLAB project ELURPGECs, as well as the TKI-PPS funding from the Dutch Ministry of Economic Affairs, HUESKER Synthetic GmbH and Ed. Züblin AG.

9 REFERENCES

Al-Tabbaa, A. and Wood, D.M., 1987. Some measurements of the permeability of kaolin. *Géotechnique*, 37(4), pp.499–514.

Prisco, C., Galli, A., Cantarelli, E. and Bongiorno, D., 2006. Geo-reinforced sand columns: Small scale experimental tests and theoretical modeling. In: *Proceedings of the 8th International Conference on Geosynthetics*. pp.1685–1688.

Raithel M., 1999. *Zum Trag- und Verformungsverhalten von geokunststoffummantelten Sandsäulen*. Kassel: Univ.-Prof. Dr.-Ing. H.-G. Kempfert.

Ardakani, A., Gholampoor, N., Bayat, M. and Bayat, M., 2018. Evaluation of monotonic and cyclic behaviour of geotextile encased stone columns. *Structural Engineering and Mechanics*, 65(1), pp.81–89.

Caicedo, B., Tristancho, J. and Thorel, L., 2015. Mathematical and physical modelling of rainfall in centrifuge. *International Journal of Physical Modelling in Geotechnics*, 15(3), pp.150–164.

Cengiz, C. and Guler, E., 2018. Shaking table tests on geosynthetic encased columns in soft clay. *Geotextiles and Geomembranes*, 46(6), pp.748–758.

Cengiz, C. and Guler, E., 2020. Load bearing and settlement characteristics of Geosynthetic Encased Columns under seismic loads. *Soil Dynamics and Earthquake Engineering*, 136.

Dipankana, B. and Viswanadham, B.V.S., 2019. Centrifuge model studies on performance of hybrid geosynthetic–reinforced slopes with poorly draining soil subjected to rainfall. *Journal of Geotechnical and Geoenvironmental Engineering*, 145(12).

German Geotechnical Society, 2011. *Recommendations for design and analysis of earth structures using geosynthetic reinforcements-EBGEO*. Berlin: Ernst & Sohn.

Poberezhnyi, V., Wittekoek, B., Van Den Berg, R., Van Eekelen, S.J.M., Cengiz, C., Detert, O., Taetz, S. and König, D., 2024. Design of centrifuge modelling of geotextile-encased column foundation systems subjected to reloading. Delft: *5th European Conference on Physical Modelling in Geotechnics (ECPMG2024)*.

Reshma, B., Rajagopal, K. and Viswanadham, B.V.S., 2019. Centrifuge model studies on the settlement response of geosynthetic piled embankments. *Geosynthetics International*, 27(2), pp.170–181.

Sharma, J.S. and Bolton, M.D., 2001. Centrifugal and numerical modelling of reinforced embankments on soft clay installed with wick drains. *Geotextiles and Geomembranes*, 19(1), pp.23–44.

Viswanadham, B.V.S. and König, D., 2004. Studies on scaling and instrumentation of a geogrid. *Geotextiles and Geomembranes*, 22(5), pp.307–328.

Zwaan, R., Terwindt, J., de Lange, D., Bezuijen, A., 2020. A new geotechnical centrifuge at Deltares, Delft, the Netherlands. *Proc. 4th European Conf. Physical Modelling Geotechnics (ECPMG 2020)*, pp 75-82.